

Ultraviolet–Ultraviolet Hole Burning Spectroscopy in a Quadrupole Ion Trap: Dibenzo[18]crown-6 Complexes with Alkali Metal Cations**

Chang Min Choi, Dae Ho Choi, Jiyoung Heo, Nam Joon Kim,* and Seong Keun Kim*

Since its first introduction more than two decades ago,^[1] ultraviolet–ultraviolet (UV–UV) hole burning (HB) spectroscopy has been extensively used for molecules and clusters produced in a supersonic jet to determine the number of different conformational isomers present in the jet as well as to obtain the conformationally selective electronic spectra.^[2–8] Conformation-selective electronic spectroscopy is crucial for the studies of large organic molecules or biomolecules in the gas phase, which generally exhibit congested and broadened spectral features because of the overlap of the vibronic peaks of different conformers.^[9,10]

In UV–UV HB spectroscopy, molecules in the first acceleration region of a time-of-flight (TOF) mass spectrometer are irradiated by a pump laser, the wavelength of which is fixed to a vibronic band of a specific conformer, to deplete the ground-state population of the conformer. After a certain time delay, a probe laser, the wavelength of which is tuned through a given spectral range, is then irradiated to ionize the molecule. Because a constant electric field is applied in the acceleration region, the ionized species by the pump or probe pulses are repelled into the field-free region of the TOF tube as soon as they are formed. The ions generated by the pump pulse arrive at the TOF detector earlier and are distinguished from those ionized by the probe pulse, even though they have the same mass-to-charge (m/z) ratio. The UV–UV HB spectrum is obtained by measuring the dip in the probe ion signal, $I_{\text{on}} - I_{\text{off}}$, where I_{on} and I_{off} are respectively the ion signals with the pump pulse on and off, as a function of the probe wavelength. Therefore, the separation of ion signals

produced by the pump and probe pulses are critical and necessary for UV–UV HB spectroscopy.

Despite the extensive use of UV–UV HB spectroscopy and its increasing importance in laser spectroscopy of larger and more flexible biomolecules in the gas phase, it has never been applied to ions in an ion trap because of the difficulty in distinguishing the ion signals produced by the pump pulse from those by the probe pulse. The fragment ions produced by the pump and probe pulses remain all trapped in the ion trap and become indistinguishable. When the direct current (DC) extraction pulse is applied on the ion trap for mass analysis, all of the fragment ions with the same m/z , irrespective of whether they are produced by the pump or probe pulses, are extracted out of the ion trap and arrive at the TOF detector with the same flight time.

In this regard, infrared (IR)–UV double resonance spectroscopy can be an alternative to UV–UV HB spectroscopy for ions in an ion trap.^[9] However, it needs to obtain the IR spectra for every vibronic band in the electronic spectrum to have the same information as the UV–UV HB spectrum, which takes much longer time and is nearly impossible for some vibronic bands of weak absorption intensity. Recently, Johnson and co-workers developed IR–IR HB spectroscopy employing an additional mass selection stage between the pump and probe pulses that are temporally and spatially separated.^[11,12] They irradiated the IR pump pulse to a particular parent ion extracted out of a quadrupole ion trap (QIT) and rejected the pump-induced photofragment ions using a mass gate in a reflectron TOF (reTOF) mass spectrometer. The fragment ions of the same parent produced solely by the IR probe pulse are then selectively detected with reTOF mass spectrometry.

Here, we introduce our new development of a simpler method of UV–UV HB spectroscopy for ions in a typical QIT–TOF mass spectrometer using only temporally separated pump and probe pulses. This method is based on our observation that some photofragment ions produced by the laser pulse do not get trapped in the ion trap but escape from it immediately after the laser pulse. By detecting those escaping ions using a reTOF mass spectrometer located next to the ion trap, we were able to distinguish the fragment ions generated by the pump pulse from those produced by the probe pulse. To demonstrate the feasibility of this method, we obtained the UV–UV HB spectra of dibenzo[18]crown-6 complexes with alkali metal cations (M^+ -DB18C6, $M = K, Rb, \text{ and } Cs$) stored in a QIT at about 10 K. DB18C6 is one of the most well-known host molecules^[13] and its complexes with alkali metal cations have recently been investigated in the gas phase using various laser spectroscopic techniques.^[14,15] By comparing the HB spectra with the corresponding photofrag-

[*] C. M. Choi, D. H. Choi, Prof. N. J. Kim
Department of Chemistry, Chungbuk National University
Cheongju, Chungbuk 361-763 (Korea)
E-mail: namjkim@chungbuk.ac.kr

Prof. S. K. Kim
Department of Chemistry and WCU Department of Biophysics and
Chemical Biology, Seoul National University
Seoul 151-742 (Korea)
E-mail: seongkim@snu.ac.kr

Prof. J. Heo
Department of Biomedical Technology, Sangmyung University
Cheonan, Chungnam 330-720 (Korea)

[**] This research was supported by the Basic Science Research Program (grant number 2010-0023857), the Star Faculty Program (grant number KRF-2005-084-C00017), the Global Frontier R&D Program on Center for Multiscale Energy System, and the World Class University Program (R31-2010-100320) through the National Research Foundation of Korea (NRF) funded by the Ministry of Education, Science and Technology.

Supporting information for this article is available on the WWW under <http://dx.doi.org/10.1002/ange.201202640>.

ment spectra, we discuss the possibility of the existence of different conformational isomers of M^+ -DB18C6.

Figure 1 shows the mass spectra of the fragment ion, K^+ , produced by photoinduced dissociation (PID) of K^+ -DB18C6

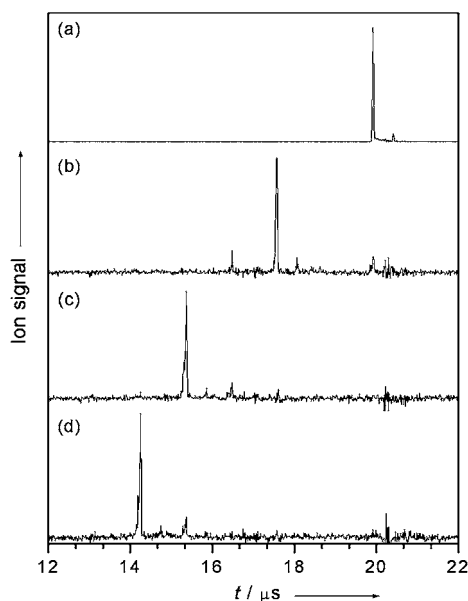


Figure 1. Mass spectra of the photofragment K^+ ion produced by PID of K^+ -DB18C6 at 274.6 nm. The laser pulse was fired after the time delays of a) 0, b) -3 , c) -5 , and d) -6 μ s from the application of the extraction DC pulse to the endcap of QIT.

at 274.6 nm.^[14] The laser pulse was fired after different time delays from the application of the extraction DC pulse to the endcap of QIT. With a time delay of 0 μ s, the K^+ ion was detected at the flight time of 19.9 μ s in the QIT-reTOF mass spectrometer. However, as the time delay was increased to -3 , -5 , and -6 μ s, the flight time decreased to 17.6, 15.4, and 14.3 μ s, respectively. The negative sign in the time delay represents that the laser pulse was fired before the application of the extraction DC pulse. Because the experimental conditions for Figure 1 are all the same and K^+ is the only fragment ion produced by PID of K^+ -DB18C6 at 274.6 nm, we assigned the ion signals in Figure 1 b–d to K^+ . Since the ions in the QIT start their flights through the reTOF tube upon application of the extraction DC pulse, the flight time of ions should not depend on the time delay between the laser and the extraction pulse. Therefore, the only explanation for Figure 1 should be that the K^+ ions begin their flights not upon application of the extraction pulse but with irradiation of the laser pulse. In other words, the ion signals in Figure 1 b–d are not due to the K^+ ions that are extracted from the QIT by the DC pulse but due to the K^+ ions that have escaped from the QIT immediately after the irradiation of the laser pulse. With the laser pulse, some of the K^+ ions produced by PID of K^+ -DB18C6 appear to escape through the hole on the exit endcap of the QIT and enter the acceleration region of the reTOF mass spectrometer, where a constant electric field is applied.

Those ions are then accelerated into the field-free region and detected by a multichannel plate (MCP). Because the laser pulse is fired before the application of the extraction pulse that defines the zero of the flight time, the K^+ ions having escaped from the QIT will be detected at a shorter flight time than those extracted by the extraction pulse. Therefore, when the time delays of the laser pulse from the extraction pulse are -3 , -5 , and -6 μ s, the decrease in flight time relative to the flight time of the pulse-extracted K^+ ions becomes -2.3 , -4.5 , and -5.6 μ s, respectively. The decrease in flight time is a little less than the corresponding time delay, which may arise from lower acceleration of the escaping ions than that of the extracted ions. The extracted ions are further accelerated inside the QIT by the electric field of the extraction DC pulse.

Interestingly, we found that the decrease in the flight time of the escaping ions is related to the period of the radio frequency (rf) signal on the QIT. Although the time delay was increased continuously, the flight time of the escaping ions decreased by a unit of 1.1 μ s ($=900$ kHz). Moreover, when the time delay was increased by less than 1 μ s, the flight time did not change from the previous value. This implies that the potential gradient formed by the rf field inside the QIT affects the escape of ions following PID.

Figure 2a shows the mass spectrum of K^+ -DB18C6 obtained by irradiating a laser pulse (probe) at 274.6 nm with a time delay of -4 μ s from the extraction pulse. The photofragment ion of K^+ is observed along with the ion signal of K^+ -DB18C6. The small ion signal at about 20 μ s arises from the K^+ ions produced by collision-induced dissociation (CID) of K^+ -DB18C6, which are then extracted by the extraction pulse.

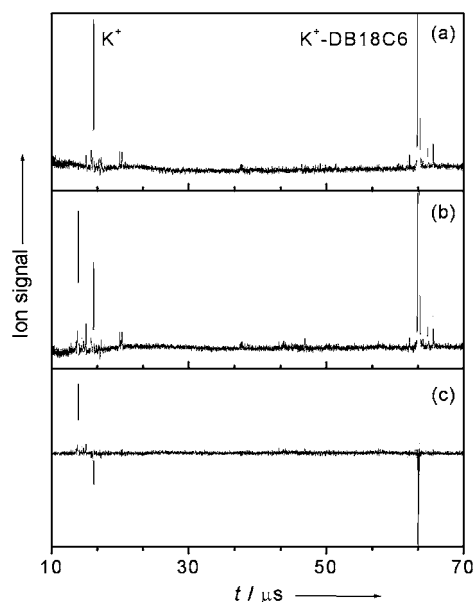


Figure 2. Mass spectra of K^+ -DB18C6 obtained by irradiation of a) the probe pulse at 274.6 nm with the time delay of -4 μ s from the extraction DC pulse, and b) both the pump and probe pulses at 274.6 nm with the time delays of -6 and -4 μ s, respectively. c) Difference mass spectrum obtained by subtracting the ion signals in (a) from those in (b).

Figure 2b is the same mass spectrum obtained by irradiating an additional laser pulse (pump) at 274.6 nm with a time delay of $-6\ \mu\text{s}$. An additional signal for the K^+ ions produced by the pump pulse appears at a little shorter flight time than the ion signal produced by the probe pulse. Moreover, the probe-induced ion signal undergoes a reduction in intensity compared to that of Figure 2a. These changes are clearly seen in Figure 2c, where the ion signals of Figure 2a are subtracted from those of Figure 2b. The positive and negative signals in Figure 2c, therefore, represent the generation and depletion of ion signals by the pump pulse. The K^+ ion signal produced by the probe pulse decreases relative to the depletion of the ground-state population of $\text{K}^+\text{-DB18C6}$ by the pump pulse.

Figure 3a shows the UV-UV HB spectrum of $\text{K}^+\text{-DB18C6}$ obtained by recording the ion dip signal of K^+ in Figure 2c as a function of the probe wavelength while fixing the pump pulse at the origin band of the transition between the ground

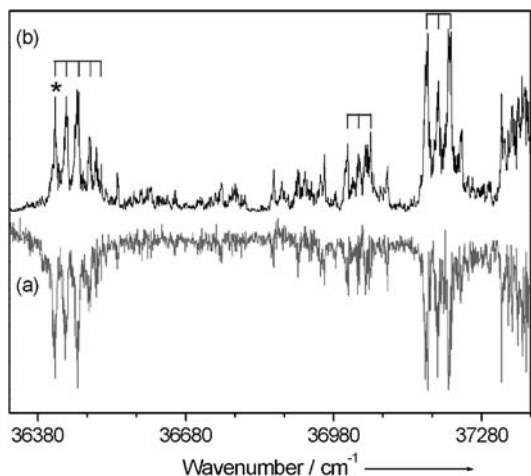


Figure 3. a) UV-UV HB spectrum of $\text{K}^+\text{-DB18C6}$ obtained by recording the dip ion signal of K^+ in Figure 2c as a function of the probe laser wavelength while the pump laser is fixed at the origin band of the $\text{S}_0\text{-S}_1$ transition (*). b) UV photofragment spectrum of $\text{K}^+\text{-DB18C6}$ obtained under the same experimental conditions.

state S_0 and the first excited singlet state S_1 .^[15] The UV photofragment spectrum of $\text{K}^+\text{-DB18C6}$ obtained by monitoring the photofragment signal of K^+ under the same experimental conditions is also shown for comparison in Figure 3b. The vibrational progression with an interval of $23\ \text{cm}^{-1}$, which was assigned previously as the butterfly mode (α), is clearly shown.^[15,16] The strong vibrational progression of the butterfly mode and its combination bands in the photofragment spectrum suggests a strong coupling of the butterfly mode with the dissociation process of $\text{K}^+\text{-DB18C6}$. All of the vibronic peaks in the photofragment spectrum of $\text{K}^+\text{-DB18C6}$ are observed in the UV-UV HB spectrum as well, indicating the presence of only a single conformational isomer in the QIT at about 10 K. The presence of a single conformer of $\text{K}^+\text{-DB18C6}$ is also consistent with the result of a previous study.^[15]

We further applied this technique to Rb^+ - and $\text{Cs}^+\text{-DB18C6}$. Unlike $\text{K}^+\text{-DB18C6}$, these complex ions are theoretically predicted to have the second lowest-energy conformers just above the most stable conformers in energy, with a difference of 0.13 and $1.4\ \text{kJ mol}^{-1}$, respectively, at the M05-2X/6-31 + G(d) level.^[15] On the basis of the IR-UV double resonance spectra, however, it was concluded that only a single conformer exists for each complex ion in the cold ion trap.^[15] But the possible existence of the other conformer was not completely ruled out because not all of the vibronic bands in the spectra were inspected by IR-UV double resonance spectroscopy. To determine whether any other conformers exist even in a minor fraction, we obtained the UV-UV HB spectra of Rb^+ - and $\text{Cs}^+\text{-DB18C6}$ by fixing the pump wavelength at the origin band of the $\text{S}_0\text{-S}_1$ transition of each complex ion (Figure 4). As in the case of $\text{K}^+\text{-DB18C6}$, all

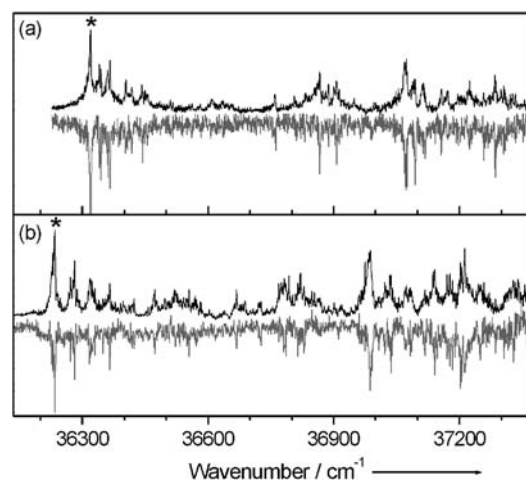


Figure 4. UV-UV HB spectra of a) Rb^+ - and b) $\text{Cs}^+\text{-DB18C6}$ obtained by fixing the pump wavelength at the respective origin bands of the $\text{S}_0\text{-S}_1$ transition. The asterisks indicate the positions of the pump wavelength. The UV photofragment spectra are also shown for comparison above the corresponding HB spectra.

of the vibronic bands in the photofragment spectra are in complete agreement with the UV-UV HB spectra, with no missing bands. On the basis of these agreements, we confirm the conclusion from the previous study^[15] that only a single conformer of Rb^+ - or $\text{Cs}^+\text{-DB18C6}$ exists in the cold QIT.

The presence of only a single conformer for each of these complex ions, contrary to the theoretical prediction for Rb^+ - and $\text{Cs}^+\text{-DB18C6}$, may be related to the method of producing those ions in the gas phase, that is, electrospray ionization (ESI). In ESI, the complex ions are first formed in solution and then brought into the gas phase through evaporation of the solvent molecules around the complex ion. Thus, if the energy barriers for isomerization to other conformers are too high for the ions to undergo isomerization during the ESI and trapping and cooling processes in the QIT, the complex ions may keep the same conformation or conformational distribution as in the solution phase. This is partially supported by our theoretical calculations on the lowest-energy conformers of Rb^+ - and $\text{Cs}^+\text{-DB18C6}$ in the gas and solution phases at the B3LYP/6-311 ++ G(d,p)//B3LYP/6-31 + G(d) level using the

conductor-like polarizable continuum model (CPCM) implemented in the Gaussian 03 suite (see the Supporting Information).^[17] We found that the energy difference between the two lowest-energy conformers of Rb^+ - and Cs^+ -DB18C6 becomes so considerable (about $2.5 \text{ kcal mol}^{-1}$) in aqueous solution that only a single conformer with C_{2v} symmetry should be dominant (see Figure S1 in the Supporting Information).

In summary, we developed a UV-UV HB spectroscopic method applicable to ions stored in a QIT. The fragment ions produced by the pump laser were distinguished from those by the probe pulse by detecting the ions escaping from the QIT immediately after the irradiation by the laser pulse for PID. The feasibility of this technique was demonstrated by obtaining the UV-UV HB spectra of K^+ -, Rb^+ -, and Cs^+ -DB18C6 stored in the QIT at about 10 K. Comparing the HB spectra with the corresponding photofragment spectra, we concluded that only a single conformational isomer exists for each complex ion in the cold QIT. This new technique will broaden the scope of conformation-selective UV-UV HB spectroscopy to ions in general, and particularly those produced by ESI, which has now become one of the most powerful tools for producing large biomolecules in the gas phase. More studies are under way to understand the ejection mechanism of photofragment ions from the QIT and its applicability to other molecular ions.

Experimental Section

The experimental apparatus is a typical QIT-reTOF mass spectrometer and the details were described elsewhere.^[14] KCl , RbCl , CsCl , and DB18C6 were purchased from Sigma-Aldrich and used without further purification. Each powder sample was dissolved in methanol to a concentration of $200 \mu\text{M}$. The DB18C6 solution was then mixed with each of the alkali metal solutions to produce a solution of M^+ -DB18C6, which was electrosprayed into ion droplets through a nozzle floated to $+3 \text{ kV}$. The solvent was removed from the ion droplets in a heated capillary and the droplets were then stored in the QIT, which was cooled to about 10 K by a closed-cycle helium cryostat.^[18,19] For the ion storage, a rf signal of a constant frequency (900 kHz) and amplitude ($+2 \text{ kV}$) was applied to the ring electrode of the QIT with its both endcaps grounded. The QIT was irradiated by the frequency-doubled output of a dye laser pumped by the third harmonic of an Nd:YAG laser as pump or probe pulses. A positive DC pulse was then applied to the entrance endcap to extract all of the ions in the QIT out

to the reTOF mass spectrometer for mass analysis. The ions were reflected by a reflectron and detected with a MCP.

Received: April 5, 2012

Published online: June 11, 2012

Keywords: electronic spectroscopy · gas-phase chemistry · laser spectroscopy · mass spectrometry

- [1] R. J. Lipert, S. D. Colson, *J. Phys. Chem.* **1989**, 93, 3894–3896.
- [2] M. S. de Vries, P. Hobza, *Annu. Rev. Phys. Chem.* **2007**, 58, 585–612.
- [3] R. K. Sinha, S. Lobsiger, S. Leutwyler, *J. Phys. Chem. A* **2012**, 116, 1129–1136.
- [4] S. Kaneko, Y. Inokuchi, T. Ebata, E. Apra, S. S. Xantheas, *J. Phys. Chem. A* **2011**, 115, 10846–10853.
- [5] S. Ishiuchi, T. Asakawa, H. Mitsuda, M. Miyazaki, S. Chakraborty, M. Fujii, *J. Phys. Chem. A* **2011**, 115, 10363–10369.
- [6] A. Abo-Riziq, L. Grace, B. Crews, M. P. Callahan, T. van Mourik, M. S. de Vries, *J. Phys. Chem. A* **2011**, 115, 6077–6087.
- [7] C. P. Rodrigo, W. H. James, III, T. S. Zwier, *J. Am. Chem. Soc.* **2011**, 133, 2632–2641.
- [8] N. Tsuji, S. Ishiuchi, C. Jouvet, C. Dedonder-Lardeux, M. Miyazaki, M. Sakai, M. Fujii, *ChemPhysChem* **2011**, 12, 1928–1934.
- [9] J. A. Stearns, S. Mercier, C. Seaiby, M. Guidi, O. V. Boyarkin, T. R. Rizzo, *J. Am. Chem. Soc.* **2007**, 129, 11814–11820.
- [10] N. S. Nagornova, T. R. Rizzo, O. V. Boyarkin, *J. Am. Chem. Soc.* **2010**, 132, 4040–4041.
- [11] B. M. Elliott, R. A. Relph, J. R. Roscioli, J. C. Bopp, G. H. Gardenier, T. L. Guasco, M. A. Johnson, *J. Chem. Phys.* **2008**, 129, 094303.
- [12] T. L. Guasco, B. M. Elliott, M. A. Johnson, J. Ding, K. D. Jordan, *J. Phys. Chem. Lett.* **2010**, 1, 2396–2401.
- [13] C. J. Pedersen, *J. Am. Chem. Soc.* **1967**, 89, 7017–7036.
- [14] C. M. Choi, H. J. Kim, J. H. Lee, W. J. Shin, T. O. Yoon, N. J. Kim, J. Heo, *J. Phys. Chem. A* **2009**, 113, 8343–8350.
- [15] Y. Inokuchi, O. V. Boyarkin, R. Kusaka, T. Haino, T. Ebata, T. R. Rizzo, *J. Am. Chem. Soc.* **2011**, 133, 12256–12263.
- [16] R. Kusaka, Y. Inokuchi, T. Ebata, *Phys. Chem. Chem. Phys.* **2008**, 10, 6238–6244.
- [17] M. J. Frisch, et al. Gaussian 03, Revision C.02; Gaussian, Inc.: Wallingford CT, **2004**.
- [18] X.-B. Wang, L.-S. Wang, *Rev. Sci. Instrum.* **2008**, 79, 073108.
- [19] M. Z. Kamrath, R. A. Relph, T. L. Guasco, C. M. Leavitt, M. A. Johnson, *Int. J. Mass Spectrom.* **2011**, 300, 91–98.